NASA Technical Memorandum 83435

Low Speed Performance of a Supersonic Axisymmetric Mixed Compression Inlet with Auxiliary Inlets

Joseph F. Wasserbauer, Robert W. Cubbison, and Charles J. Trefny
Lewis Research Center
Cleveland, Ohio

Prepared for the
Nineteenth Joint Propulsion Conference
cosponsored by the AIAA, SAE, and ASME
Seattle, Washington, June 27-29, 1983

NASA

LOW SPEED PERFORMANCE OF A SUPERSONIC AXISYMMETRIC MIXED COMPRESSION INLET WITH AUXILIARY INLETS

Joseph F. Wasserbauer, Robert W. Cubbison,
and Charles J. Trefny

National Aeronautics and Space Administration
Lewis Research Center
Cleveland, Ohio 44135

ABSTRACT

A research program was conducted to determine the aero/acoustic performance of a representative supersonic cruise inlet. The discussion herein is limited to inlet aerodynamic performance. A fan simulator was coupled to the inlet to provide characteristic noise signatures and to pump the inlet flow. Data were obtained at Mach numbers from 0 to 0.2 for the inlet equipped with an auxiliary inlet system that provided 20 to 40 percent of the fan flow. Results show that inlet performance improved when the inlet bleed systems were sealed; when the freesteam Mach number was increased; and when the auxiliary inlets were opened. The inlet flow could not be choked by either centerbody translation or by increasing the fan speed when the 40 percent auxiliary inlet was incorporated.

E-1730

INTRODUCTION

Supersonic cruise inlets are designed to provide optimum performance at cruise conditions. As a result, the inlet cowl lip is sharp, bleed systems are incorporated in the design and the inlet capture area is smaller than that required at takeoff conditions. Therefore, auxiliary inlet systems are necessary to provide the additional engine airflow that is required at takeoff. These additional openings in the inlet nacelle provide additional paths for propagation of fan generated noise. Acoustic analysis, references 1 to 3, shows that forward propagated fan noise would be a prominent noise component at both takeoff and approach conditions. Aerodynamically, because of the internal flow characteristics of supersonic inlets at low speeds, large performance penalties could result from lip flow separations, reference 4, and from inflow bleed. Reduction of inlet performance penalties and reduction of aircraft generated noise to the surrounding community are of paramount importance.

Reductions in propagated fan noise levels could be accomplished through inlet choking techniques and careful design of auxiliary inlet systems. Use of variable geometry techniques could reduce lip flow separation and improve inlet performance. Experimental verification of these techniques and design concepts at ground static and low speed conditions would be of utmost importance to insure that overall inlet performance is not compromised.

A schematic of an axisymmetric translating centerbody inlet shown in figure 1(a), illustrates the various aero/acoustic phenomena that may be present at static , takeoff, and approach conditions. The top half of the sketch shows the inlet with the centerbody extended and auxiliary inlets full open providing maximum flow area in the inlet. Air flows into the inlet through the main inlet duct, and through the auxiliary inlets. Because of the cowl's

sharp lip, internal flow separation is encountered at the inlet cowl lip. Low internal duct static pressures serve to pump additional flow into the inlet through the cowl and centerbody bleed systems. This inflow bleed increases the compressor face distortion which decreases the engine stall margin. Also, fan generated noise propagates to the surrounding environment through the inlet main duct and open auxiliary inlets.

The lower half of the sketch illustrates several techniques to maintain inlet aero/acoustic performance at ground static and low speed conditions. Aerodynamically, retracting the centerbody reduces the cowl lip Mach number which minimizes lip flow separation. Sealing the inlet bleed systems prevents reverse airflow into the inlet duct and eliminates a possible source of increased flow distortion. Acoustically, inlet choking to reduce noise propagation is accomplished by reducing the inlet throat area (centerbody retracted) and the auxiliary inlet area. Each of these inlet conditions could increase flow distortion. Acoustic treatment of the inlet internal surfaces could also enhance the inlet acoustic attenuation.

Before the termination of the Supersonic Cruise Research (SCR) effort by NASA, a program was initiated to acquire test data on the aero/acoustic performance of a supersonic cruise inlet at speeds representative of takeoff and landing operations. An initial test was conducted with a supersonic cruise aircraft at ground-static conditions (ref. 5). Results indicated significant reduction in noise level even though the inlet duct could not be choked. Preparations continued for a more comprehensive test using an existing well instrumented inlet model that is representative of typical flight hardware. Particular attention was paid to aerodynamic performance and noise transmission aspects of auxiliary inlet system concepts. The effects of forward speed, sharp lip flow separations, bleed system back-flow, and realistic auxiliary inlet-flow distortions were considered of fundamental importance to the investigation.

Participants in this program were NASA Lewis and NASA Langley and the three SCR contractors, Boeing, Lockheed, and Douglas. Each participant (except NASA Langley) was to design, fabricate, and test auxiliary inlet systems that would be representative of their auxiliary inlet concepts and be adapted to the existing inlet model system. The NASA-Ames P-inlet model was selected for this investigation. Its design is representative of proposed supersonic cruise inlet designs, and auxiliary inlet systems could be easily accommodated. The inlet system was coupled to a JT8D refan simulator powered by an air turbine. The fan simulator provided characteristic fan noise signatures and pumped the airflow through the inlet. The objective of the program was to test each design to determine experimentally its aerodynamic and acoustic performance.

The inlet system was mounted in the NASA-Lewis 9x15-ft anechoic wind tunnel. Test data were obtained at freestream Mach numbers of 0 to 0.2. The fan simulator was operated at corrected speeds ranging from 40 percent to 90 percent of rated speed.

This paper presents a summary of the aerodynamic performance obtained during the NASA-Lewis portion of the program, (which is the only portion of the program which has been completed to date).

APPARATUS AND PROCEDURE

The inlet used in the investigation is the NASA-Ames P-inlet. This is a mixed-compression inlet designed for a cruise Mach number of 2.65. The inlet

is an axisymetric, translating centerbody design with a cowl lip diameter of 49.723 cm. The model size is approximately 1/3 scale of an inlet suitable for application on a supersonic transport. This inlet model was previously tested over a range of Mach numbers from mid-subsonic to its design supersonic cruise Mach number. The results of these tests are reported in references 6 to 8. A photograph of the model installed in the 9x15-ft anechoic wind tunnel is shown in figure 1(b). The microphone array was used to record the far field noise signatures eminating from the inlet model. The acoustic results of the NASA-Lewis investigation are reported in reference 9.

Figure 2 shows a schematic of the test inlet model. Both internal and external contours are representative of flight hardware. Cowl and centerbody internal aerodynamic contours are listed in tables I and II of reference 8. Originally, the model had a remotely operable centerbody and bypass doors. For the test reported herein, only the centerbody position was varied to change internal flow conditions and inlet throat area. The bypass door sections were modified to accept the various auxiliary inlet systems. The model also features multiplenum boundary layer bleed systems for the cowl and the centerbody. Various bleed hole patterns could be used, however, only bleed pattern 4 of reference 8 was used. The cowl bleed pattern is fixed. The centerbody has a traveling bleed system, and a detailed description is found in reference 8. Both cowl and centerbody bleed systems are representative of flight systems and any inflow bleed would be representative of actual conditions.

Inlet area variation with centerbody translation is shown in figure 3. Throughout the test only five centerbody positions were used from fully extended to fully retracted. These positions are indicated on figure 3. Aerodynamic and acoustic data were obtained at each of these centerbody positions.

A schematic of the inlet model coupled to the JT8D refan simulator including total pressure rakes and dynamic pressure instrumentation locations is shown in figure 4. The NASA-Lewis JT8D refan simulator (refs. 10 and 11), was selected to provide the pumping characteristics and noise signatures that would be representative of a Variable Cycle Engine (VCE). A transition section coupling the inlet to the JT8D refan simulator was necessary because of the slight difference in mating internal duct diameters. The transition length was maintained as short as possible based on aerodynamic considerations.

The model instrumentation consisted of inlet total pressure rakes mounted at the cowl lip, throat, and compressor face stations. The cowl lip rake had two static probes included in the rake to aid in calculation of cowl lip Mach number. Surface static pressure taps were located along the cowl and centerbody internal surfaces. Their locations are identified in tables 11 and 12 of reference 8. The JT8D refan simulator had total pressure rakes installed in the inlet guide vanes and downstream of the exit stators in both the bypass duct and core duct. Dynamic pressure transducers were located on the cowl and centerbody and used to determine noise propagation characteristics through the inlet duct. During a contractor test phase, a traversing total pressure probe was mounted downstream of the inlet throat to survey the duct flow from cowl to centerbody at the various centerbody translated positions. Selected total pressure profiles will be presented in this report.

Compressor face instrumentation detail is shown in figure 5. A total of twelve total pressure rakes were used to determine the compressor face flow characteristics. Static pressure taps were located at the hub and tip of each rake and on the side walls of the struts. Therefore, each quadrant was completely instrumented. The compressor face station was used as the flow

measuring station. Combination steady state-dynamic total pressure probes were installed in rakes located at 45, 135, 225, 315 degrees to measure the dynamic content of the compressor face flow.

The NASA-Lewis designed auxiliary inlet configurations are shown in figure 6. The entrance flow area was designed to provide 20 and 40 percent of the inlet cowl lip area. Static pressure taps were located along the centerline of the auxiliary inlet ramp and aft lip surfaces. A cover plate was fixed over the 40 percent auxiliary inlet entrance when a closed auxiliary inlet configuration was tested. A photograph of the 40 percent auxiliary inlet system is shown in figure 7. The inlet guide vanes of the JT8D refan simualtor are visible through the auxiliary inlet entrance.

Inlet data were obtained by first selecting a fan corrected speed with the centerbody at its fully extended position. The centerbody was then retracted to each of the four additional preselected positions (see fig. 3). Aerodynamic data was recorded for each centerbody position while acoustic data recording was more selective. Another fan speed value was set and the process repeated until inlet choking conditions or fan stall limits were reached. Data were recorded at these limits.

Since the JT8D refan simulator could pump more airflow than the design airflow for the P inlet (equivalent VCE airflow), a relationship is required to equate the JT8D refan test corrected speeds to typical VCE corrected speeds. To provide this relationship a JT8D refan speed was selected that provided a model compressor face Mach number representative of a typical VCE value at takeoff throttle condition, (compressor face Mach number of 0.6). This JT8D refan corrected speed was then defined as "100 percent VCE fan equivalent design speed." Table I lists the values of JT8D refan corrected speeds used during the test program and their equivalent VCE percent design corrected speeds. Throughout this paper, test data will be presented as fan equivalent design speed.

The tests were conducted in the NASA-Lewis 9x15-ft anechoic wind tunnel at freestream Mach numbers of 0, 0.1, and 0.2. A freestream Mach number of 0.2 is a maximum tunnel condition.

RESULTS AND DISCUSSION

Effect of Bleed, Auxiliary Inlets Closed

Inlet performance at a freestream Mach number of 0.2 with the auxiliary inlets closed is shown in figure 8. Performance comparisons are made for inlet configurations with full open bleed systems and with the bleed systems sealed. At a given fan corrected speed, the inlet throat Mach number was varied by retracting the centerbody from full extend, ($\Delta X/RL = 1.57$), to full retract, ($\Delta X/RL = 0$). Throat Mach numbers were calculated by using the lowest value of the throat region static pressure measured along the cowl centerline to the average throat rake total pressure. A simple Mach number pressure ratio relationship was then used.

Inlet pressure recovery over the inlet operating range for the open bleed configuration was from 1 to about 6 percent below the pressure recovery for the sealed bleed configuration. Also, inlet distortion increased more rapidly with open bleeds and varied from 2 to 14 percent greater than the distortion for the sealed bleed configuration.

For the sealed bleed configuration, inlet choking conditions were nearly reached with the centerbody in the full retracted position at a fan equivalent

design speed of 73 percent. Here the pressure recovery and distortion were about 0.87 and 0.19, respectively. Inlet choking conditions were realized for fan equivalent design speeds of 86 and 93 percent at centerbody positions of $\Delta X/R1$ of 0.8 and 1.57 (full extend), respectively. At these conditions, pressure recoveries were about 0.89 and distortions about 0.16. Data show that surface Mach numbers greater than 1.0 were recorded. This means that the flow expanded beyond the inlet throat. No fan stalls were encountered with the bleeds closed.

With the bleed systems open, the centerbody could be fully retracted only for fan equivalent design speeds of 46 and 59 percent. However, for fan equivalent design speeds of 73 and 86 percent, the centerbody could be retracted only 60 percent of its travel to a $\Delta X/RL$ of 0.64. Fan stall limits were encountered at a centerbody position of $\Delta X/RL$ of 0.64 for fan equivalent design speeds of 73 and 86 percent because of high distortion caused by the reverse bleed flow. Inlet choking conditions were not realized because of the fan stall limitations. At the stall limit for the fan equivalent design speed of 73 percent, the pressure recovery was 0.91 with a distortion of 0.19. At a fan equivalent design speed of 86 percent, the stall limit pressure recovery was about 0.85 and the distortion about 0.30. A fan equivalent design speed of 93 percent was not attemped due to the high distortion at 86 percent speed.

A sample of the total pressure profiles throughout the inlet duct at a centerbody position of $\Delta X/RL$ of 0.8 is shown in figure 9. Data are compared for inlet configurations with and without bleed at a freestream Mach number of 0.2 and fan equivalent design speed of 73 percent. This data is for a throat Mach number of about 0.75. Traversing probe data is included here and defines the total pressure profile from cowl to centerbody just downstream of the throat rake. The effect of inflow bleed from the cowl bleed system is shown in all profiles from the throat rake to the compressor face rake, figure 9. Air inflow through the bleed system distorts the profile at the cowl surface at the throat station and this low pressure region persists at the compressor face rake. Traversing probe data shows evidence of the low energy inflow bleed on the cowl and flow separtion off the centerbody. The effect of inflow bleed on the centerbody is difficult to determine because of the inherent centerbody flow separation. With the bleeds sealed, the influence of the centerbody separation appears to dominate and the high pressure is near the cowl at the compressor face rake.

Total pressure contours at the compressor face station for a fan equivalent design speed of 73 percent are shown in figure 10. The contours were constructed for each compressor face quadrant to provide more realistic flow visualization for an inlet system with support struts ahead of the compressor face. The total pressure contours were constructed for each quadrant by using the measured static pressures on the cowl, hub and strut sidewalls as the boundaries. The rake total pressures were then faired radially and circumferentially to obtain the proper contours. Characteristic of all the cortour plots are the pressure gradients in the strut region, and a four per rev flow pattern that an engine would experience. Four per rev flow patterns are not necessarily bad and in some cases, engines have shown more tolerance to this flow pattern than was previously anticipated, reference 12. The magnitude and extent (circumferential) of the pressure gradients in the strut regions could be contributing factors to engine tolerance for this type of flow pattern.

Total pressure contours for the conditions of figure 9 are shown in figure 10(a). With inlet bleeds open, the higher pressure region is nearer the centerbody. Also, there appears to be some asymmetry in this contour pattern. When the inlet bleed system is sealed, a fairly symmetrical pattern

results. The influence of the centerbody separation is seen in the hub region as noted above. Here, the contour shaping suggests that the centerbody flow separation tends to be channeled to the center of each quadrant at the hub surface.

With bleed systems sealed, the inlet was operated near a choked condition for a centerbody position of $\Delta X/RL$ of 0 at a fan equivalent design speed of 73 percent. The total pressure contour for this condition is shown in figure 10(b). As noted above, the high pressure collected at the cowl as a result of the strong influence of the centerbody flow separation. Pressure lobes in the strut corners of the cowl show possibility of vortex flow formation. At this full retract position of the centerbody, the distortion was near 20 percent, however, no fan stall was encountered.

The total pressure contour at the fan stall limit for the open bleed system configuration and fan equivalent design speed of 73 percent is shown in figure 10(c). The influence of the cowl inflow bleed again dominates and the high pressure is near the centerbody. A hint of asymmetry at the stall condition is also noted.

From the results of figures 8 to 10, it appears that the design of a supersonic cruise inlet should have provisions to prevent inflow bleed during low speed operation with the auxiliary inlets closed. Design of inlet bleed systems, which incorporate divices to prevent inflow bleed, may be a formidable task.

During the test program when auxiliary inlets were open, data were obtained with the bleed systems opened and closed. However, the remaining data presented in this report will be for inlet performance with sealed bleed systems.

Inlet Performance With Auxiliary Inlets

The effect of varing auxiliary inlet entrance area at a freestream Mach number of 0.2 is shown in figure 11. No fan stalls were encountered. Inlet choking could be accomplished with closed auxiliary inlets, as was noted above, and also with the 20 percent auxiliary inlet configuration. The data with auxiliary inlets closed (fig. 11(a)), is reported in figure 8. For the 20 percent auxiliary inlet configuration, inlet choking did not occur until a fan equivalent speed of 100 percent was reached (fig. 11(b)). At this fan speed, inlet choking occured when the centerbody was retracted to a position of $\Delta X/RL$ of 0.4. At a fan equivalent design speed of 113 percent, inlet choking occurred at a centerbody position of $\Delta X/RL$ of 1.00.

The inlet could not be choked when the 40 percent auxiliary inlets were employed even when the fan was operated at a fan equivalent design speed of 113 percent, figure 11(c). As a result, the inlet throat area could be varied over the complete range without choking, (centerbody translation from $\Delta X/RL = 1.57$ to 0.0).

In general, the pressure recovery variation with throat Mach number was nearly the same for the open auxiliary inlets with the 40 percent configuration slightly higher. The pressure recovery for the closed auxiliary inlet configuration varied from about 1 to 3 percent below open auxiliary inlets. However, when comparisons are made at the same fan equivalent design speeds, differences are noted. For example, with the 40 percent auxiliary inlet and a fan equivalent speed of 100 percent, the pressure recovery varied from 0.98 to 0.97 as the throat Mach number was increased (fig. 11(c)). With the 20 percent auxiliary inlets at the same speed, the pressure recovery varied from 0.95 to 0.91 for increasing throat Mach numbers (fig. 11(b)). This would be

expected since the throat Mach numbers vary from 0.69 to a choke condition for the 20 percent auxiliary inlets, a more severe inlet operating range. The 40 percent auxiliary inlets only operated from throat Mach numbers of 0.5 to about 0.72.

For all three auxiliary inlet configurations, distortion values were less than 0.10 for throat Mach numbers less than 0.75. At fan equivalent design speeds of 100 percent, the highest distortion recorded for the 40 percent auxiliary inlets was 0.10 while for the 20 percent auxiliary inlets, the highest distortion recorded was about 0.19 (an inlet choke condition).

In general, at a freestream Mach number of 0.2, the pressure recovery and distortion are influenced more by the inlet throat Mach number and less by the auxiliary inlet entrance area.

Total pressure profiles throughout the inlet duct for the various auxiliary inlet configurations are presented in figure 12. Data are compared for a centerbody position of $\Delta X/RL$ of 0.8 and a fan equivalent design speed of 73 percent at a freestream Mach number of 0.2. The lip rake total pressure profiles show that with the auxiliary inlets closed, some lip flow separation is evident. As the auxiliary inlets are opened, lip flow separation is considerably reduced for the 20 percent auxiliary inlets and little evidence of lip flow separation is seen when the auxiliary inlets are opened to 40 percent. The differences in static pressures at the throat rake illustrates the change in Mach number as the auxiliary inlets are opened. Also noted is the diminishing influence of the lip flow separation on throat profiles as the auxiliary inlets are opened. At the compressor face rake station, the total pressure profile for the closed auxiliary inlet shows the influence of the centerbody flow separation, as noted above. The total pressure profiles for the 20 percent and 40 percent auxiliary inlets appear to be fairly flat. However, the influence of the slip flow between the auxiliary inlet flow and the main duct flow is seen by the slight depression in the profiles at radius ratios of 0.8 and 0.7 for the 20 percent and 40 percent auxiliary inlets respectively. It also appears that the centerbody flow separation has a slight influence on the total pressure profile for the 20 percent auxiliary inlet.

Compressor face total pressure contours for the three auxiliary inlet configurations of figure 12 are presented in figure 13. It is interesting to note the difference in the strut contour patterns when the auxiliary inlets are opened and closed. With the auxiliary doors closed, smooth contour lines are seen along the strut side walls, while with open auxiliary inlets the contour lines are influenced by the slip flow between the main duct and auxiliary inlet flows. As noted above, when the auxiliary inlets are closed, the centerbody flow separation influences the flow near the hub.

Effect of Mach Number on Lip Flow Separation

Effect of freestream Mach number on lip flow separation for the three auxiliary inlet configurations is presented in figure 14 for a fan equivalent design speed of 73 percent. Presented in the figure are cowl lip rake total pressure profiles and respective cowl lip Mach numbers for each auxiliary inlet configuration. A Mach number was calculated for each total pressure probe on the rake that was not immersed in the separated region. These Mach numbers were then averaged and are presented in the figure. Data for centerbody positions of 1.57 and 0 are presented. In general, the extent of lip flow separation is reduced as the freestream Mach number is increased for all data presented in figure 14.

In figure 14(a), for a centerbody position of 1.57, data show that the radial extent of lip flow separation is reduced as freestream Mach number is increased. However, only the auxiliary inlet opening of 40 percent shows the lip flow separation nearly eliminated at a freestream Mach number of 0.2. At this condition, the cowl lip Mach number is about 0.3.

At a centerbody position of 0, no lip flow separation is observed for all configurations at a freestream Mach number of 0.2 (fig. 14(b)). For all three configurations, it is noted that the cowl lip Mach number is lower than 0.23. However, lip flow separation persists for all auxiliary inlet configurations at the ground-static condition (Mo = 0). For a freestream Mach number of 0.1, lip flow separation is nearly gone for the 40 percent auxiliary inlet configuration but remains for the 20 percent and the closed auxiliary inlet configuration. It is noted that as the cowl lip Mach number is reduced to values between 0.2 and 0.25, the lip flow separation begins to wane.

In general, as the freestream Mach number is increased, the radial extent of the lip flow separation is reduced. Increasing auxiliary inlet opening, and retracting the centerbody, decreases lip flow separation until cowl lip Mach numbers approach values of 0.2 to 0.25. It appears that when a freestream Mach number of 0.2 is reached and the cowl lip Mach number approaches this value, cowl lip flow separations are minimized or eliminated.

Internal cowl static pressure distributions for various auxiliary inlet configurations and centerbody positions are shown in figure 15. Data are presented for an equivalent fan design speed of 73 percent at a freestream Mach number of 0.2.

For a centerbody position of 1.57, the aerodynamic throat is clearly defined at the cowl lip station for all three auxiliary inlet configurations (fig. 15(a)). The cowl lip separation modifies the inlet's geometric area variation in the region of the cowl lip. Based on one dimensional inviscid calculations and the area distribution for $\Delta X/RL$ of 1.57 (fig. 3), a minimum pressure ratio was obtained at the cowl lip for each auxiliary inlet configuration's pressure distribution. The dashed lines on figure 15(a) represents the projection of the data if no separation were present. It appears that the linear extent of lip flow separation could be defined as the juncture of the dashed line and data for each pressure distribution. When the auxiliary inlets are closed, the separated flow appears re-attached to the cowl at a model station of about 3.2. As the auxiliary inlets are opened, re-attachment moves forward to the cowl lip. For the 40 percent auxiliary inlet configuration re-attachment occurs at a model station of about 2.7.

When the centerbody is fully retracted, no lip separation is evident at the cowl lip and the aerodynamic throat is defined at a model station of about 4.3 (fig. 15(b)). The static pressures at the compressor face station (model station 7.2) show that as the auxiliary inlets are opened, the main duct flow and the flow from the auxiliary inlets are accelerated to the compressor face Mach number as determine by the fan speed. The difference in the static pressures for the three auxiliary inlet configurations are a result of difference in total pressure recovery for the various configurations. The slight depression in the static pressure distributions at a model station of about 5.4 is due to the localized flow acceleration around the strut leading edge. In general, opening auxiliary inlets and retracting the centerbody reduces the linear extent of lip flow separation.

Auxiliary Inlet Performance

Static pressure distributions on the ramp and lip surfaces of the auxiliary inlets are presented in figure 16 for 73 and 100 percent fan equivalent

design speeds. Data are presented for two centerbody positions and at a freestream Mach number of 0.2. At a centerbody position of 1.57, the static pressure distribution is nearly the same for the 20 and 40 percent auxiliary inlet configurations. The ramp static pressures show the gradual increase in flow velocity as the airflow is channeled into the auxiliary inlet. The lip static pressure distribution shows that the stagnation point is near the lip high lite with an acceleration zone just downstream on the internal lip surface. The flow continues to accelerate into the auxiliary inlet channel with another acceleration zone at the entrance into the main duct, model station 7.05. This static pressure distribution is characteristic of the auxiliary inlets for various centerbody positions and fan equivalent design speeds.

As the centerbody is retracted and the fan speed increased, the Mach number in the lip acceleration zone increases as well as the Mach number in the acceleration zone at the entrance into the main duct. The acceleration zone at the main duct corner entrance indicates supersonic flow has been attained (fig. 16(a)). This localized supersonic flow on the cowl just downstream of the auxiliary inlet could serve to impede the propagation of any noise that is generated by high fan tip speeds. Thus a source of fan noise reduction is possible if the design of auxiliary inlets could produce localized sonic or supersonic conditions at high engine airflow without deterioration of inlet performance.

SUMMARY

A supersonic cruise inlet whose design is representative of typical flight hardware was tested for aero/acoustic performance in the NASA Lewis 9x15 ft anechoic wind tunnel at ground-static conditions, and at freestream Mach numbers of 0.1 and 0.2. Supersonic cruise inlets require auxiliary inlets at the low speed takeoff conditions in order to provide the airflow that the engine demands. The selected aerodynamic data, presented and reported herein, were obtained to determine the effect of inflow bleed on inlet performance when the auxiliary inlets were closed, and the effect of open auxiliary inlets with the inlet bleed system sealed. This performance data was also obtained to aid in defining the acoustic characteristics of a typical supersonic cruise inlet.

The results of this investigation are as follows:

Inlet operation with the auxiliary inlets closed shows that the inlet could be choked when the bleed systems were sealed. Operation with the bleed systems opened caused inflow bleed, which increased distortion such that fan stall limits were reached before inlet choking could occur.

With the inlet bleed system sealed, good performance was obtained with the 20 and 40 percent auxiliary inlet openings. The inlet could be choked with the 20 percent auxiliary inlet but only at fan equivalent design speeds of 100 and 113 percent.

Increasing the freestream Mach number reduces the radial extent of the lip flow separation. At a freestream Mach number of 0.2, cowl lip flow separation is minimized or eliminated when cowl lip Mach numbers approach values of 0.2 obtained by either centerbody translation, increasing auxiliary inlet opening, or a combination of the two.

High airflow into the auxiliary inlets produced localized supersonic conditions at the cowl surface juncture of the auxiliary inlet and main duct. This localized sonic or supersonic condition could provide an acoustic impedence to any propagation of fan noise to the surrounding environment.

APPENDIX - SYMBOLS

A	local duct area
ACL	cowl lip area = 0.1942 sq.m (300.981 sq.in.)
DISTA	compressor face distortion = (P1max - P1min) /P2
Mo	freestream Mach number
ML	cowl lip Mach number
Mt	throat Mach number
P2	average compressor face total pressure
Po	freestream total pressure
P1	local total pressure
p	static pressure
RL	cowl lip radius = 24.862 cm (9.788 in)
r	radius
X	Axial distance from theoretical tip of centerbody at $\Delta X = 0$
ΔX	forward translation of centerbody from theoretical retracted cruise position

REFERENCES

1. Technology Application Study of a Supersonic Cruise Vehicle, NASA CR 159276, Douglas Aircraft, March 1980.
2. Supersonic Cruise Vehicle Technology Assessment Study of an Over/Under Engine Concept, NASA CR 159247, Lockheed-California Company, January 1980.
3. Advanced Concept Studies for Supersonic Vehicles, NASA CR 159244, Boeing Commercial Airplane Company, May 1980.
4. Fradenburgh, Evan A., and Wyatt, DeMarquis D., Theoretical Performance Characteristics of Sharp-Lip Inlets at Subsonic Speeds, NACA TN 3004, Sept. 1953.
5. Bangert, L.H.; Burcham, Jr., F. W. ; and Mackall, K. G. ; "YF-12 Inlet Suppression of Compressor Noise: First Results", AIAA-80-0099, Aerospace Sciences Meeting, January 14-16, 1980.
6. Koncsek, J. L. and Syberg, J., "Transonic and Supersonic Test of a Mach 2.65 Mixed Compression Axisymmetric Intake", CR 1977, March 1972, NASA.
7. Smelter, Donald B. and Sorensen, Norman E., "Analytical and Experimental Performance of Two Isentropic Mixed Compression Axisymmetric Inlets at Mach Numbers 0.8 to 2.65", TN D-7320, June 1973, NASA.
8. Syberg, J. and Turner, L. "Supersonic Test of a Mixed Compression Axisymmetric Inlet at Angles of Incidence", CR 165686, April 1981, NASA.
9. Woodward, Richard P.; Glaser, Frederick W.; Lucas, James G.; Low Flight Speed Acoustic Results for a Supersonic Inlet with Auxiliary Inlet Doors", AIAA Paper AIAA-83-1415, June 1983.
10. Moore, Royce D.; Kovich, George; and Tysl, Ed ard R., "Aerodynamic Performance of 0.4066 Scale Model of JT8D Refan Stage", NASA TM X-3356, March 1976.
11. Moore, Royce D.; Kovich, George; and Lewis, George W. Jr.; "Aerodynam Performance of 0.4066-Scale Model of JT8D Refan Stage with S-Duct Inl NASA TN D-8458, May 1977.
12. King, R. W., Schuerman, J. A., and Muller, R. G., "Analysis of Distor n Data From TF30-P-3 Mixed Compression Inlet Test", NASA CR-2686, June 1976.

TABLE I. -

JT8D refan corrected speeds	VCE fan equivalent design corrected speed, percent
40	46
50	59
60	73
70	86
75	93
80	100
90	113

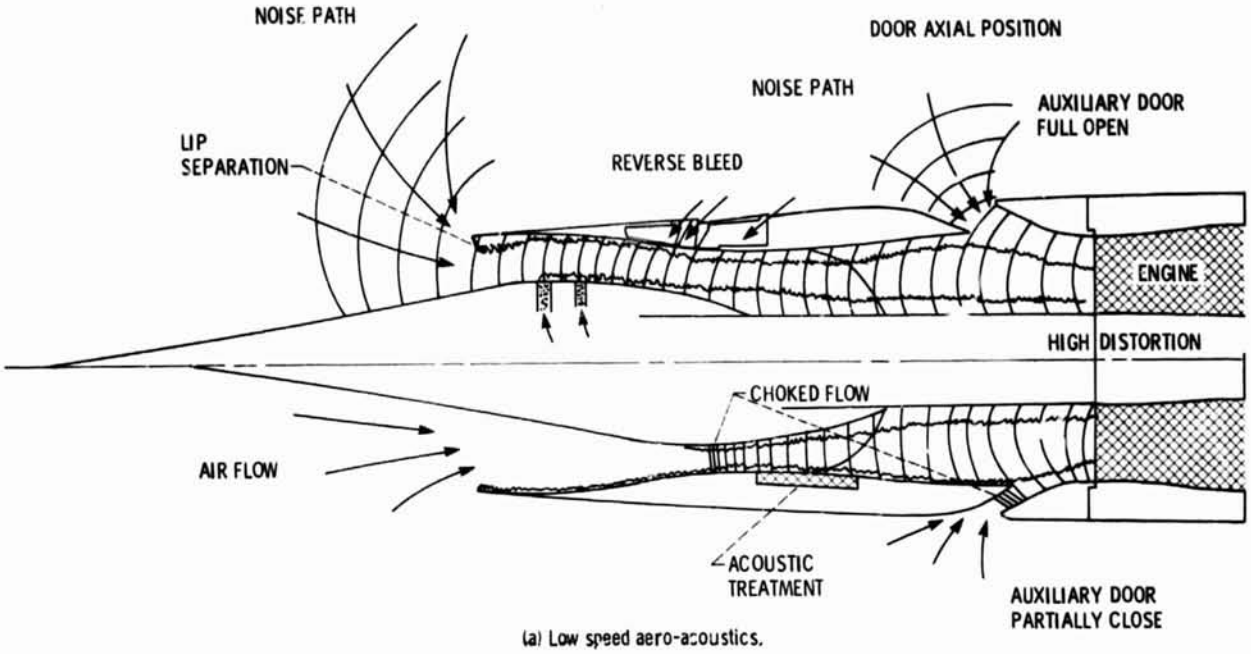

(a) Low speed aero-acoustics.

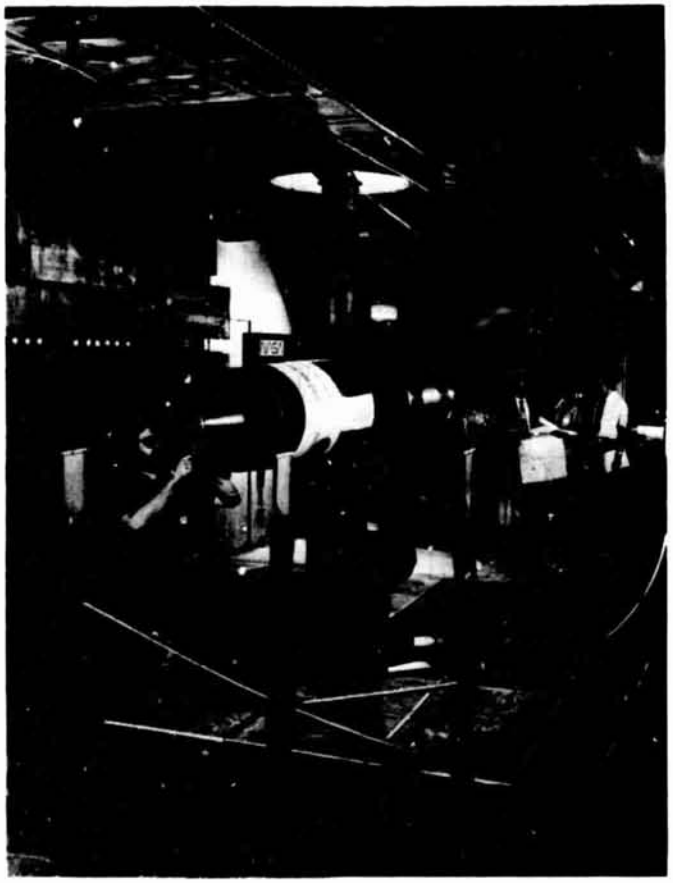

(b) Modified P-inlet with auxiliary inlets installed in the 9x15 ft wind tunnel.

Figure 1. - Low speed aero-acoustics test.

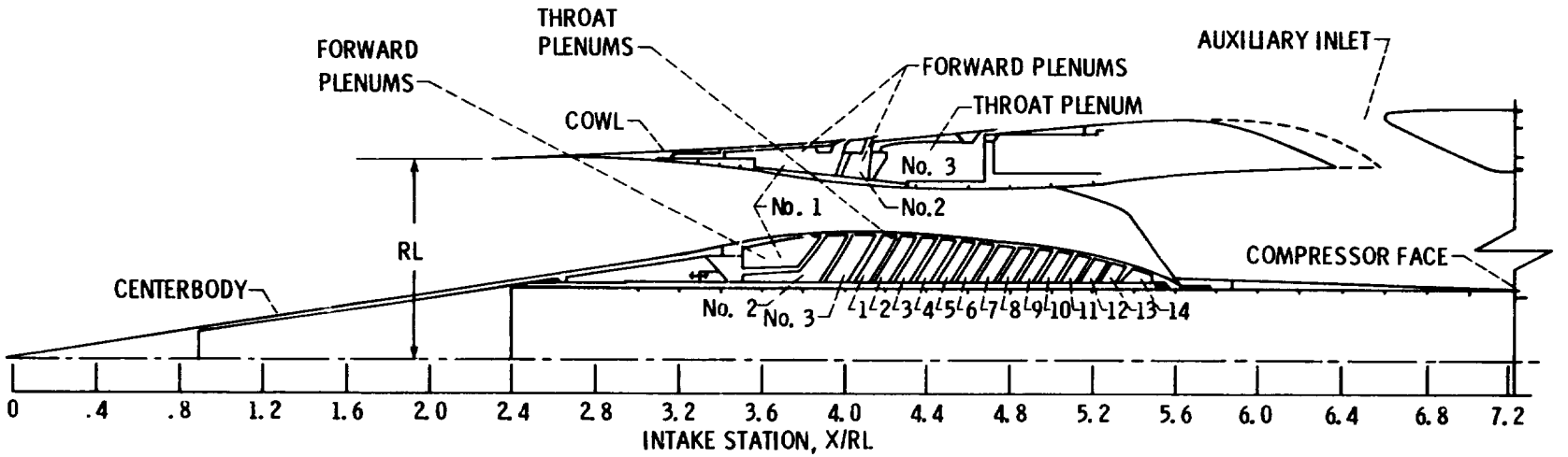

Figure 2. - Model Schematic.

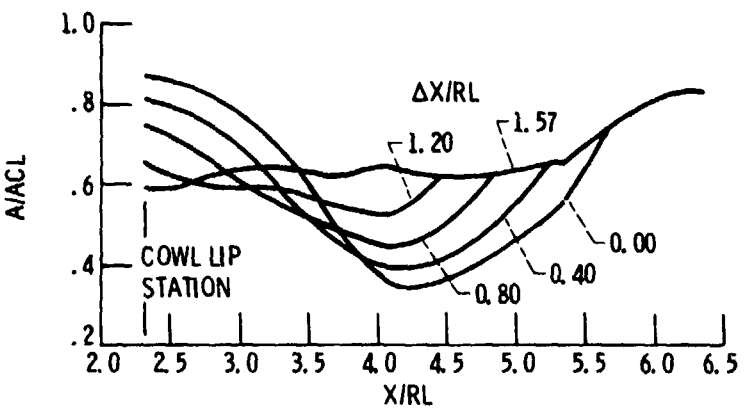

Figure 3. - Inlet area variation.

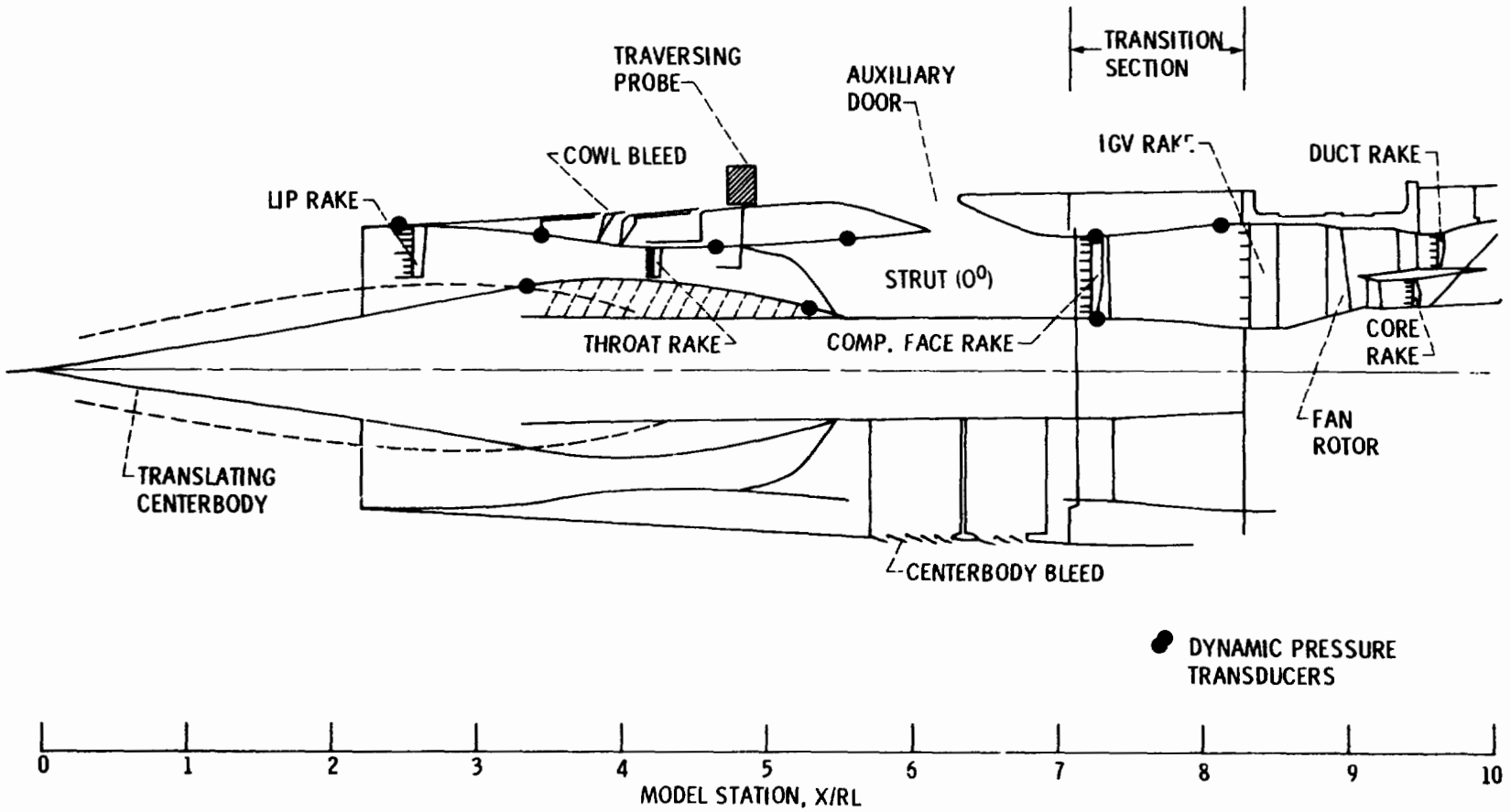

Figure 4. - Modified P-inlet and fan simulator instrumentation.

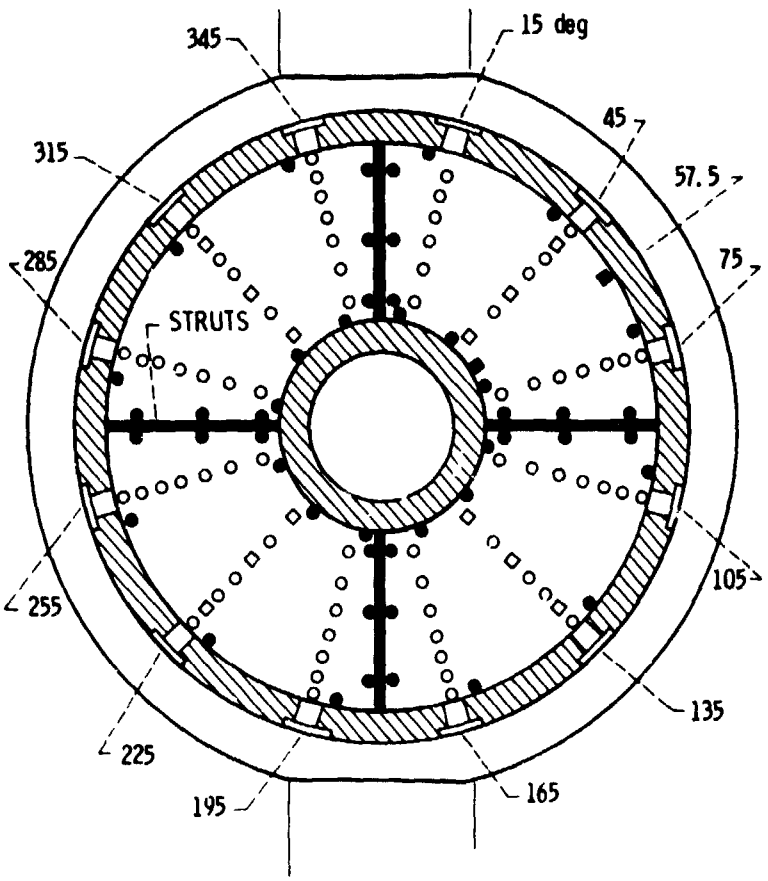

- STATIC PRESSURE (COWL, CENTERBODY, STRUTS)
- DYNAMIC PRESSURE TRANSDUCERS (STATIC)
- COMBINATION DYNAMIC AND STEADY-STATE TOTAL PRESSURE PROBE
- TOTAL PRESSURE

Figure 5. - Compressor face instrumentation.

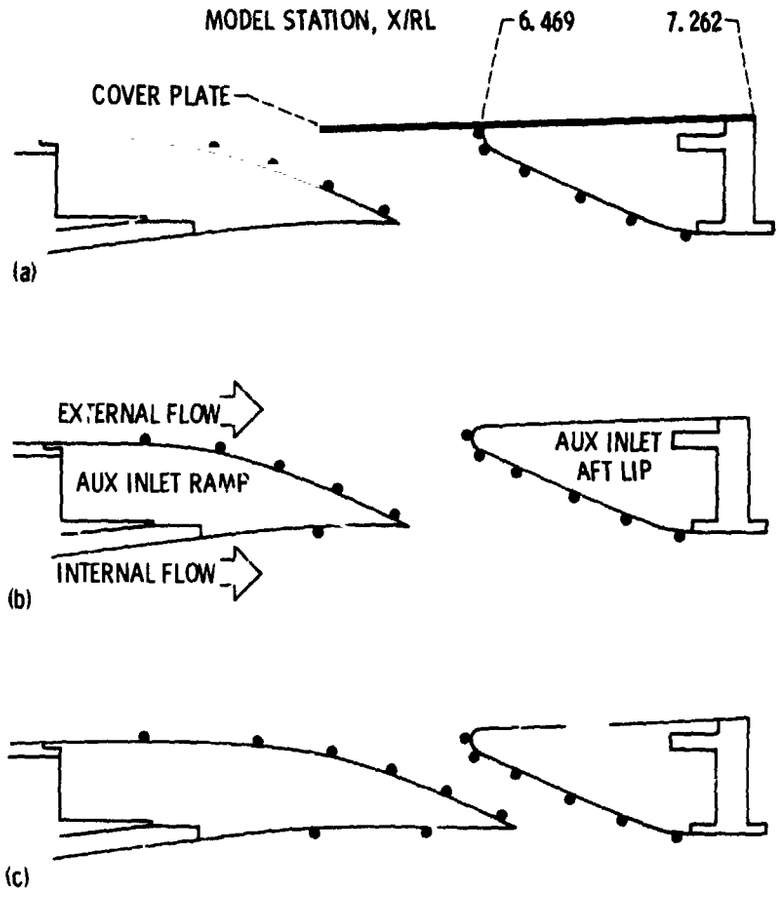

(a) Auxiliary inlet closed.
(b) 40% ACL auxiliary inlet opening.
(c) 20% ACL auxiliary inlet opening.

Figure 6. - Auxiliary inlet configurations.

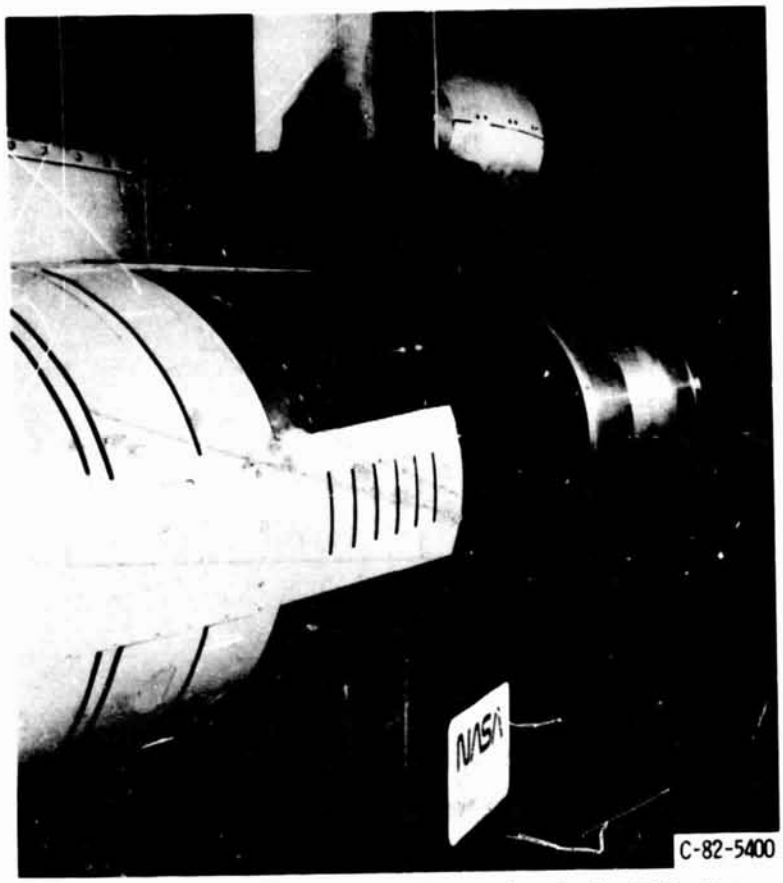

Figure 7. - Model with 40% auxiliary door opening showing JT8D refan simulator.

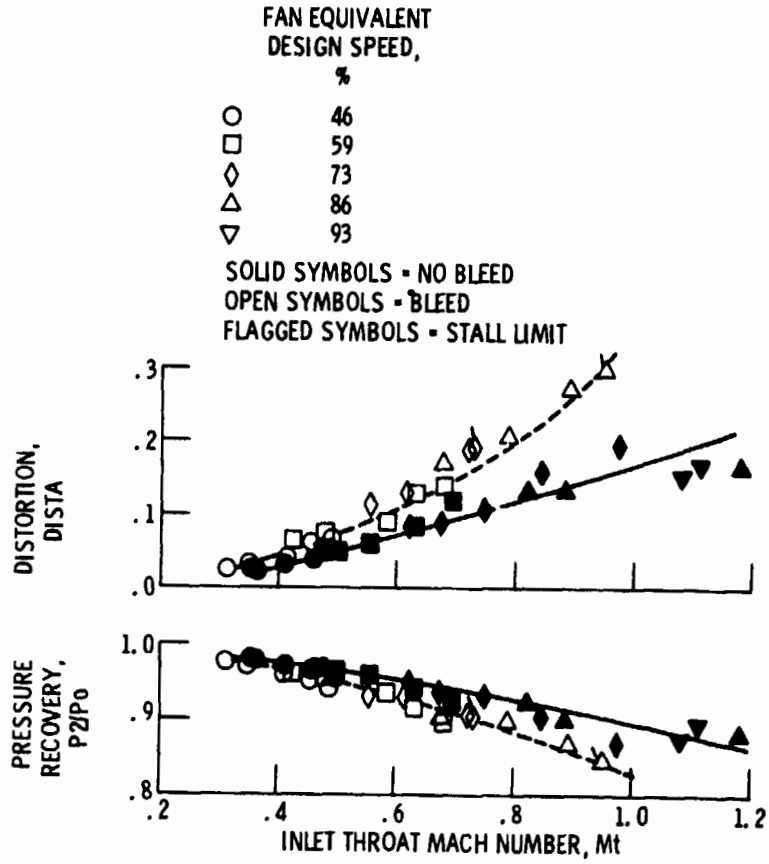

Figure 8. - Effect of inflow bleed on inlet performance with auxiliary inlets closed. $M_0 = 0.20$.

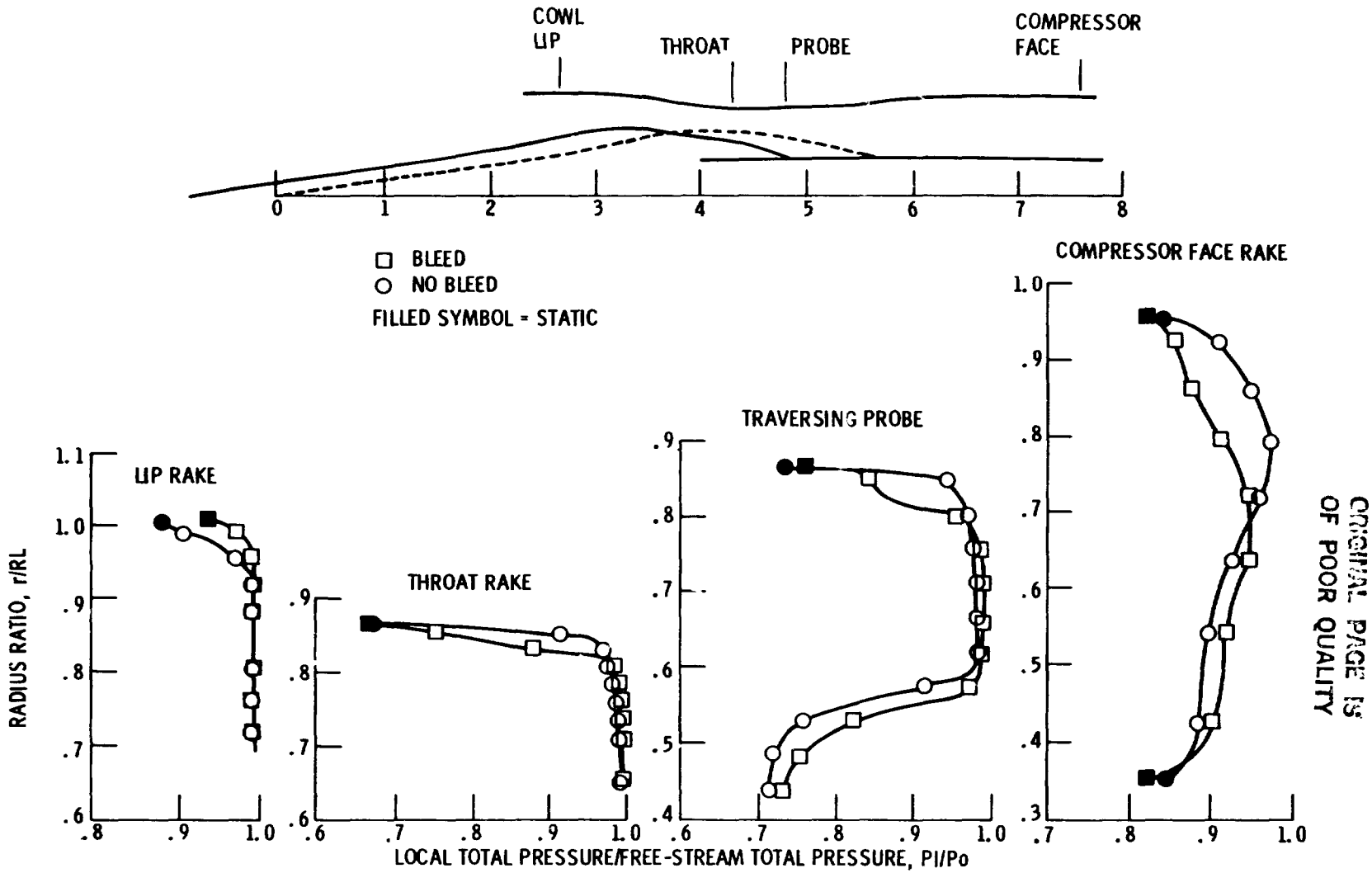

Figure 9. - Inlet duct total pressure profiles, auxiliary inlets sealed, 73% fan equivalent design speed, $M_0 = 0.2$, $\Delta X/RL = .8$.

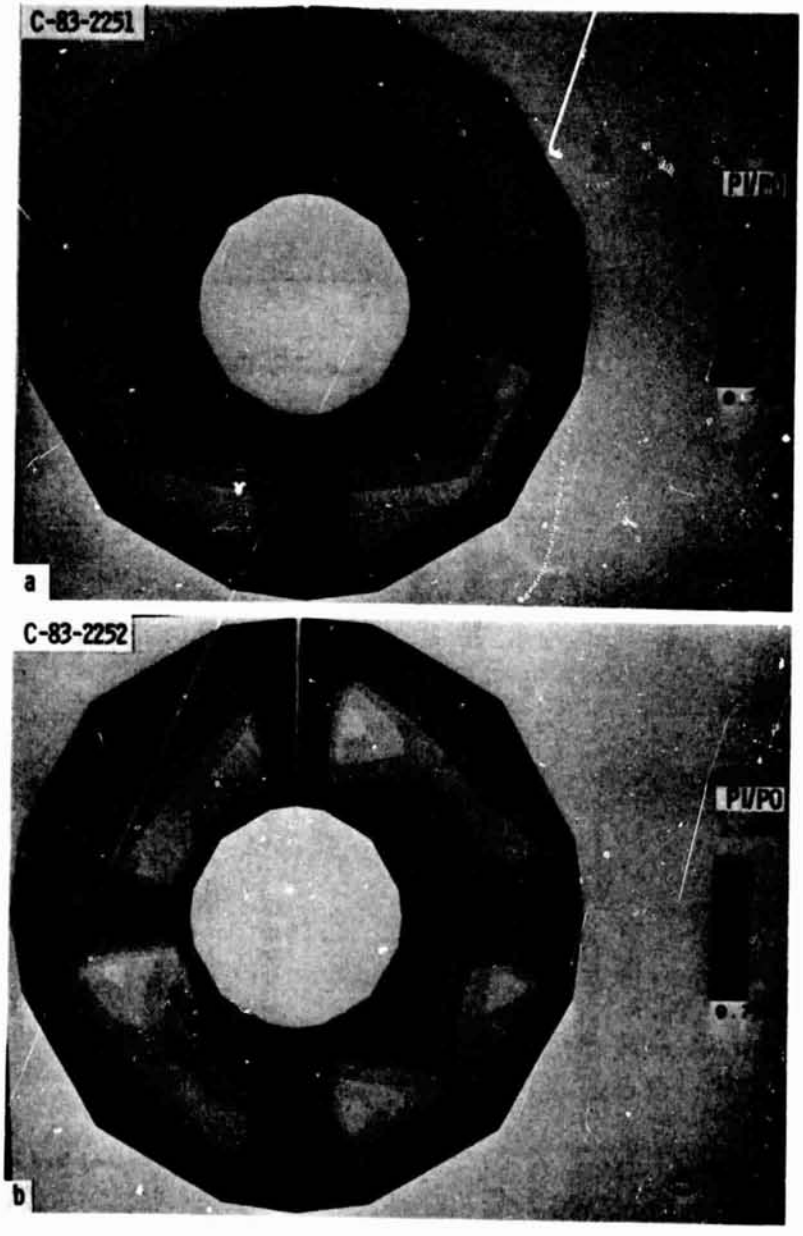

(a) Cowl and centerbody bleeds sealed. DISTA = 0.108 P2/P0 = 0.932.
(b) Cowl and centerbody bleeds open. DISTA = 0.192 P2/P0 = 0.909.
$\triangle X/RL = 0.8$

Figure 10. - Compressor face total pressure contours, auxiliary inlets sealed, 73 percent fan equivalent design speed, $M_0 = 0.2$.

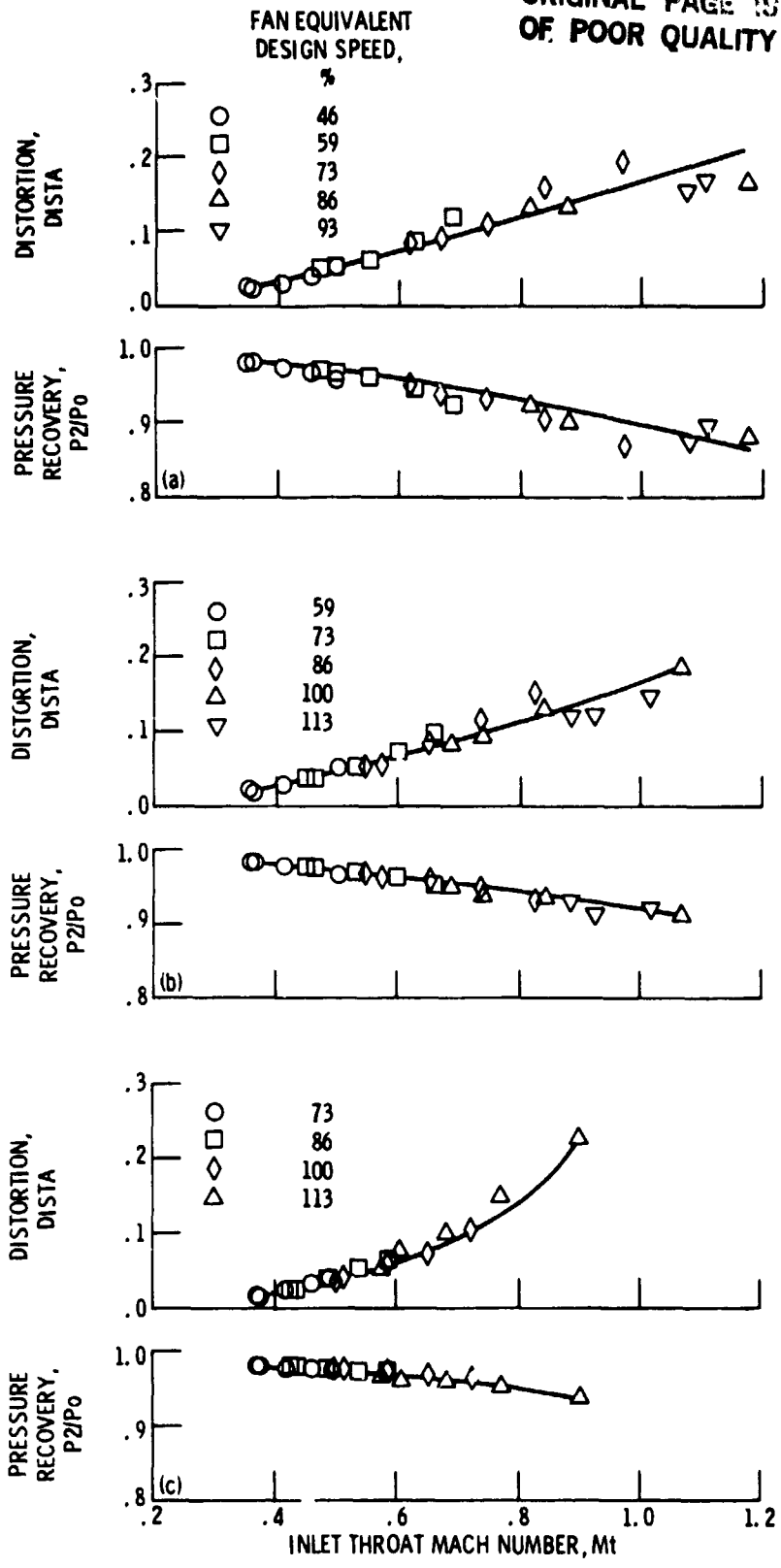

(a) Auxiliary inlets closed.
(b) 20% auxiliary inlets.
(c) 40% auxiliary inlets.

Figure 11. - Effect of auxiliary inlets on inlet performance with inlet bleed systems sealed. M_0 = 0.20.

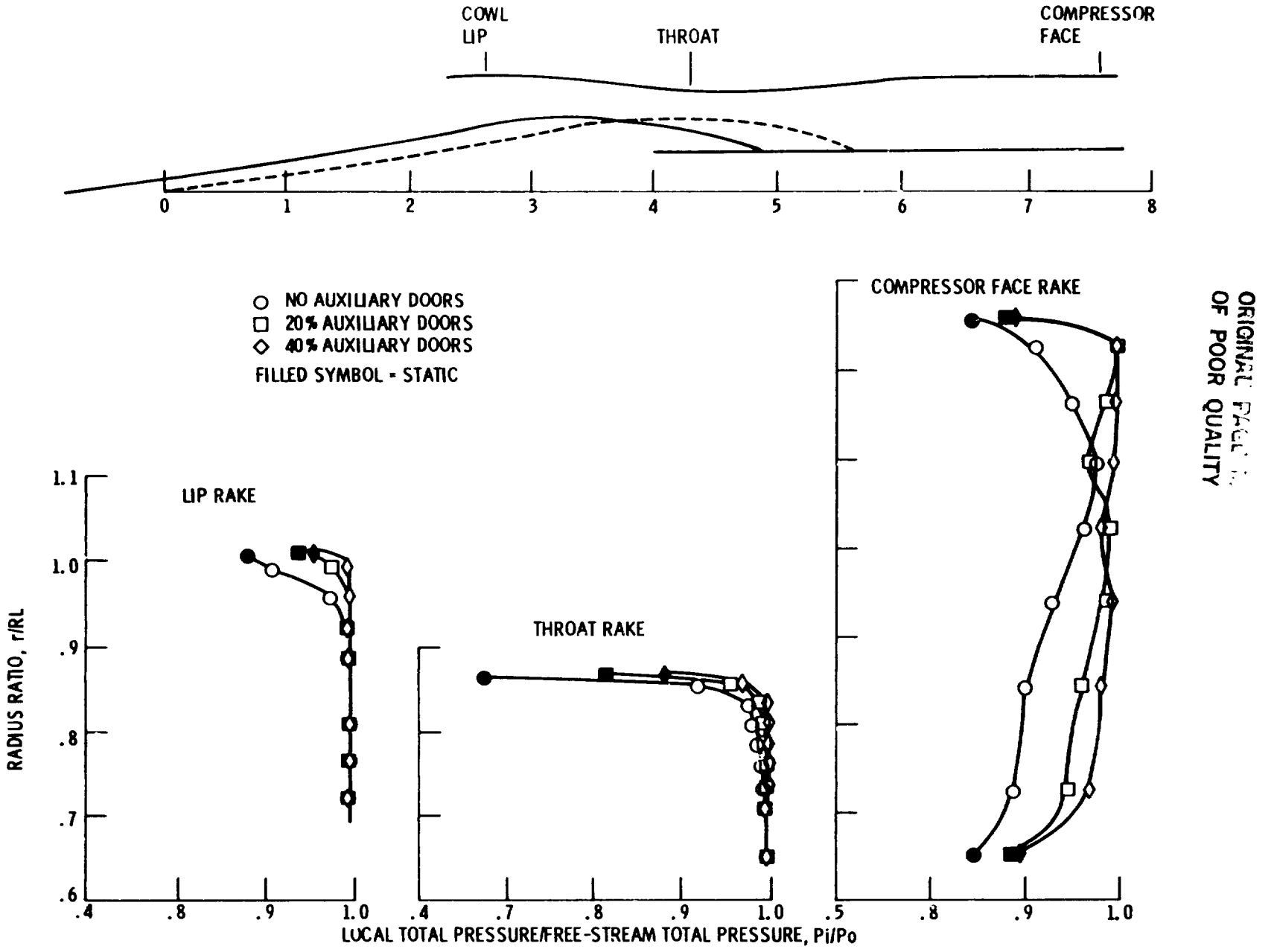

Figure 12. - Inlet duct total pressure profiles, 73% fan equivalent design speed, bleed systems sealed, $\Delta X/RL = 0.8$, $M_0 = 0.20$.

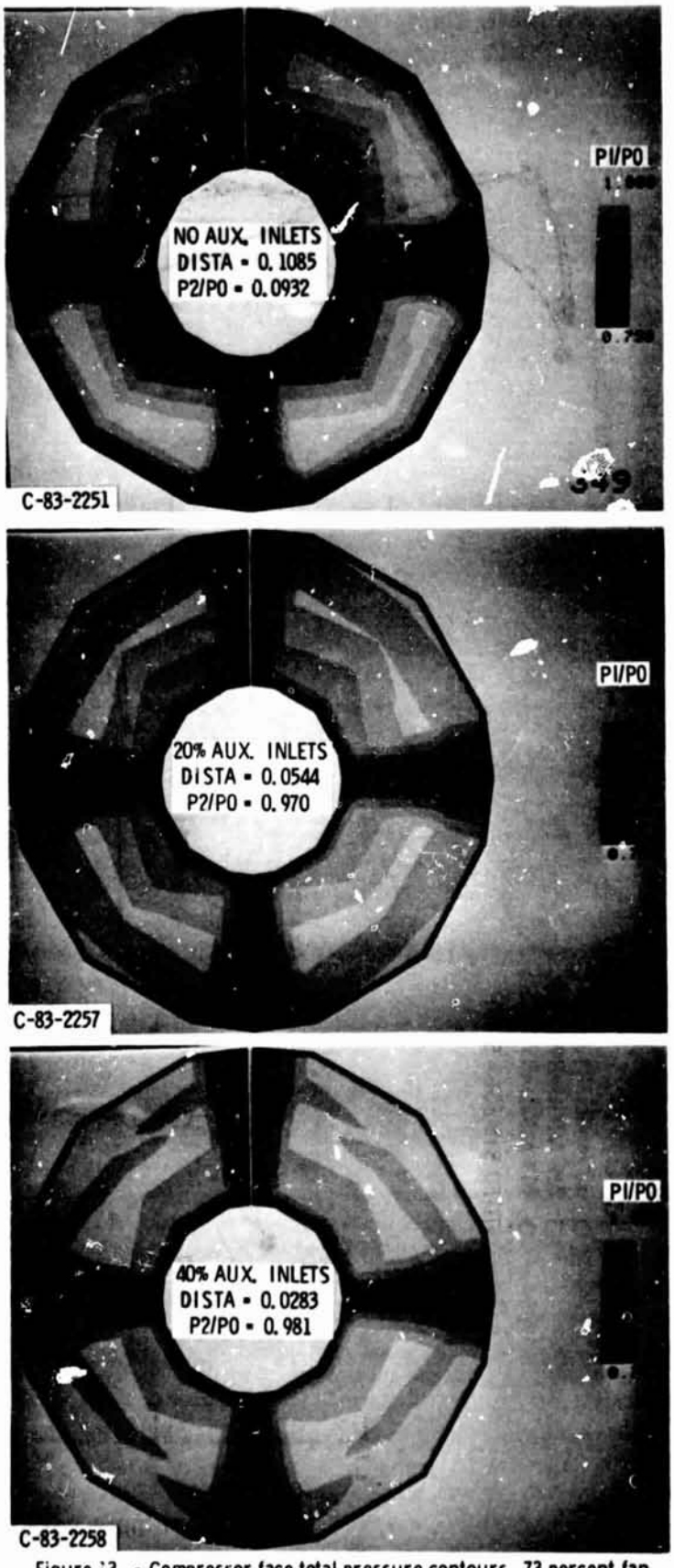

Figure 13. - Compressor face total pressure contours, 73 percent fan equivalent design speed, bleed system sealed, $M_0 = 0.2, \Delta X/RL = 0.8$.

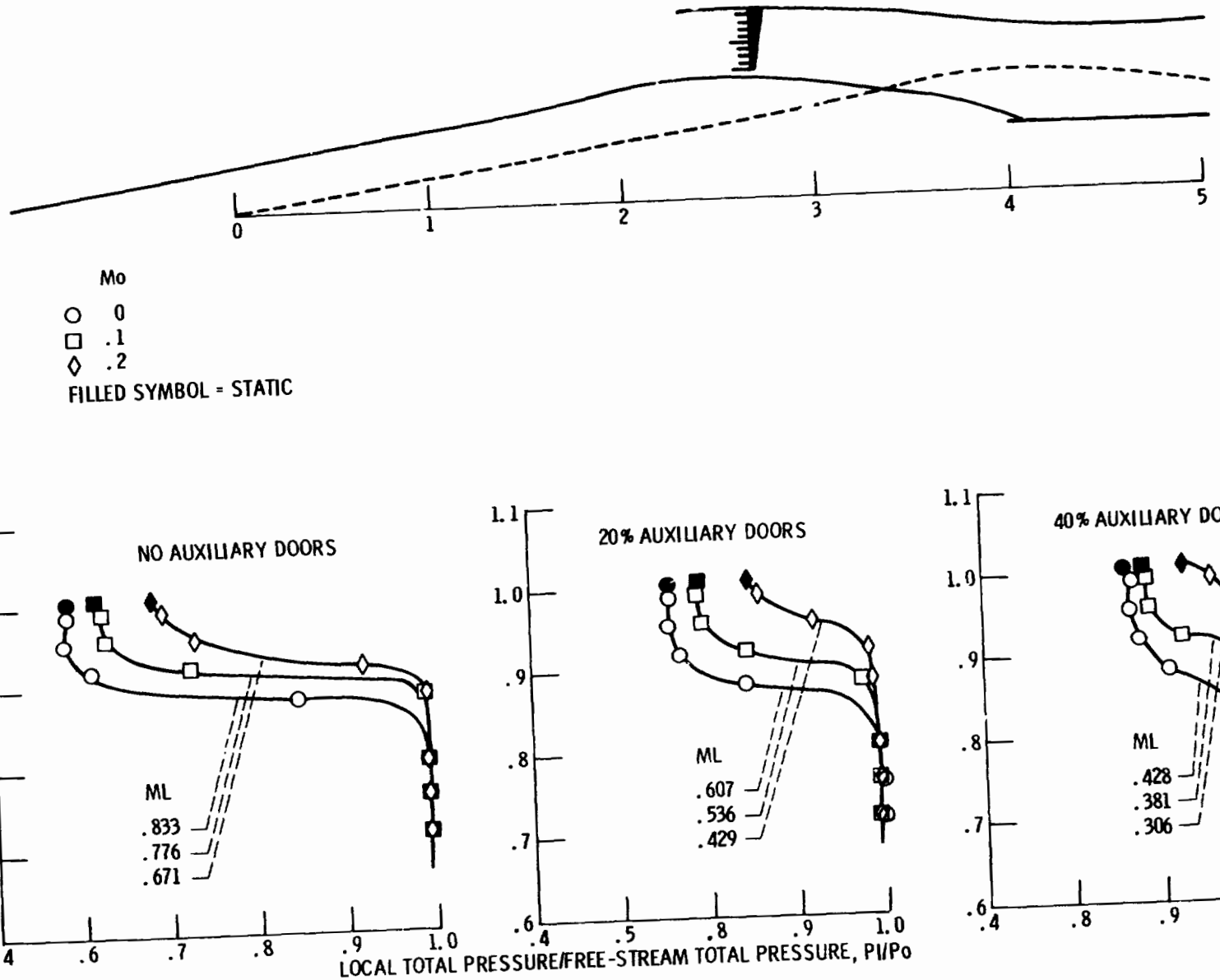

(a) ΔX/RL = 1.57.

Figure 14. - Effect of free-stream Mach number on lip separation, 73% fan equivalent design speed.

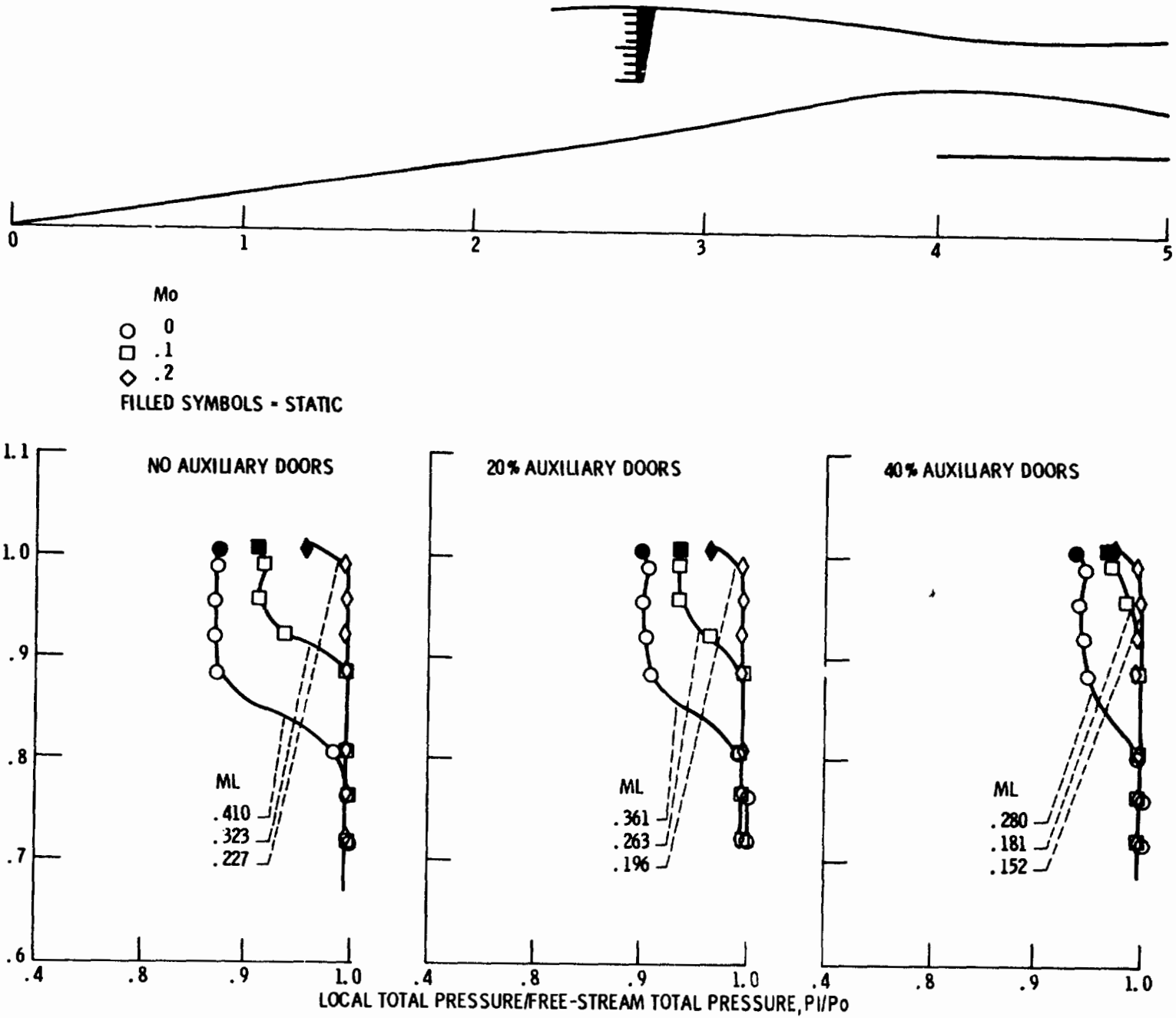

(b) $\Delta X/RL = 0$.

Figure 14. - Concluded.

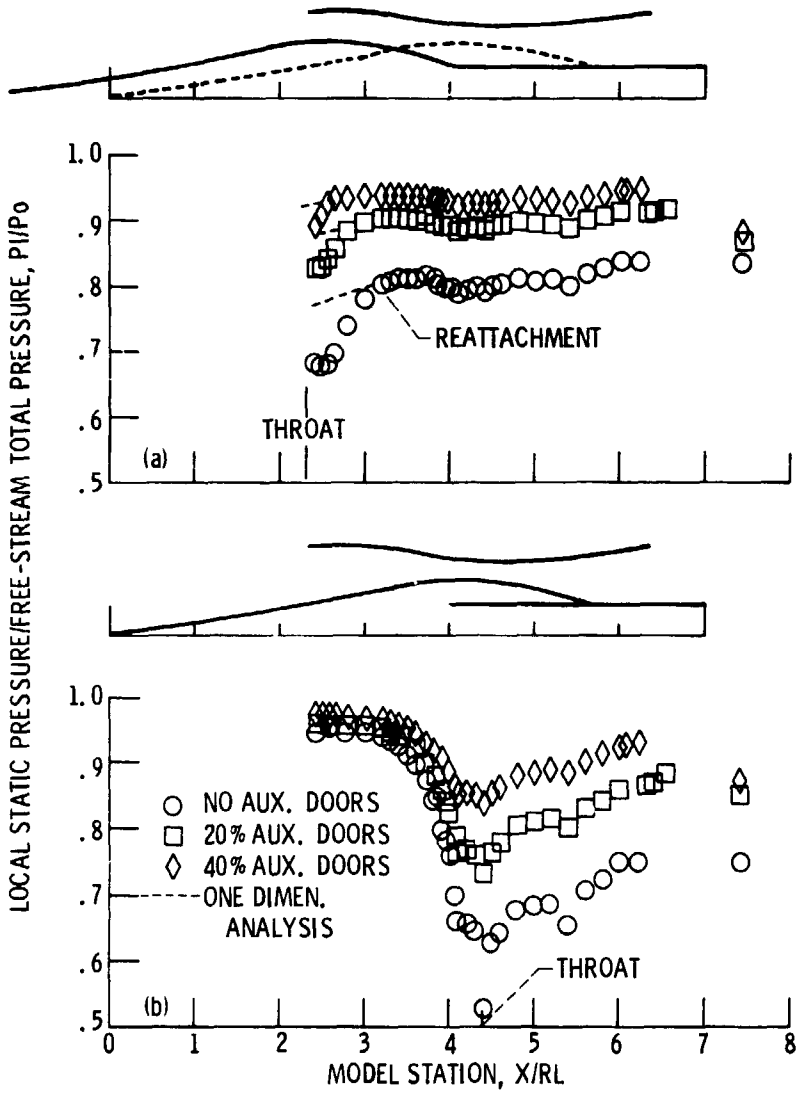

(a) ΔX/RL = 1.57
(b) ΔX/RL = 0.

Figure 15. - Internal cowl static pressure distribution for various auxiliary inlet settings and centerbody positions, bleed systems sealed, 73% fan equivalent design speed, M_0 = 0.20.

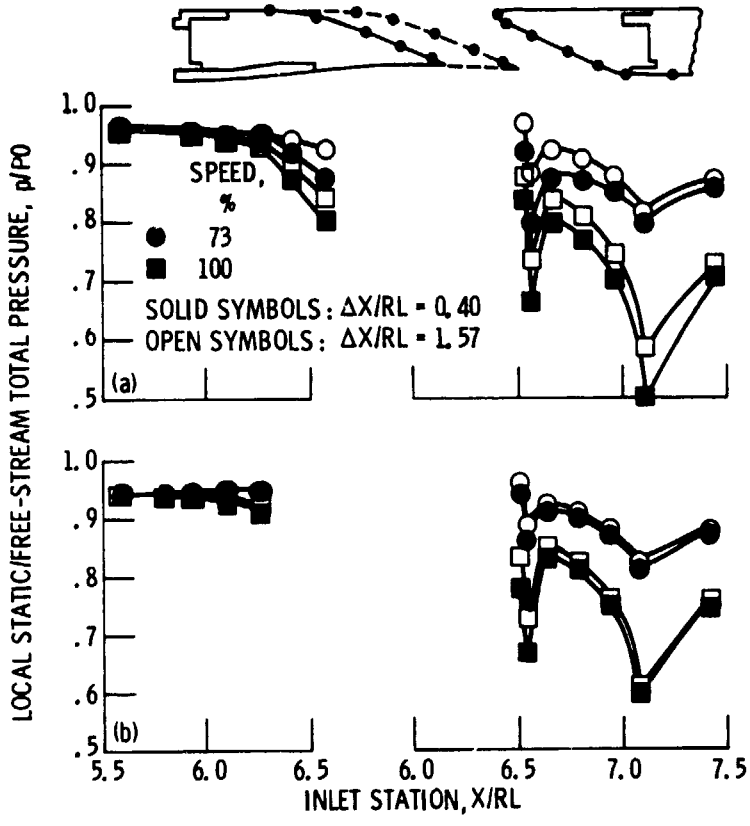

(a) 20% auxiliary doors
(b) 40% auxiliary doors.

Figure 16. - Auxiliary inlet static pressure distributions for various fan speeds and centerbody positions. No bleed, Mo = 0.20.